Published in final edited form as:
Fertil Steril. 2015 January ; 103(1): 270–280.e8. doi:10.1016/j.fertnstert.2014.09.023.

Granulocyte colony-stimulating factor prevents loss of spermatogenesis after sterilizing busulfan chemotherapy

Roberto Benavides-Garcia[1,3], **Rose Joachim**[1,3], **Nancy A. Pina, BS**[1], **Kazadi N. Mutoji, PhD**[1], **Matthew Reilly, PhD**[2], and **Brian P. Hermann, PhD**[1,4]

[1]Department of Biology, The University of Texas at San Antonio, One UTSA Circle, San Antonio, TX 78249.

[2]Department of Biomedical Engineering, The University of Texas at San Antonio, One UTSA Circle, San Antonio, TX 78249.

Abstract

Objective—To determine if granulocyte colony-stimulating factor (G-CSF) could prevent loss of spermatogenesis induced by busulfan chemotherapy via protection of undifferentiated spermatogonia, which might serve as an adjuvant approach to preserving male fertility among cancer patients.

Design—Laboratory animal study.

Setting—University.

Animals—Laboratory mice.

Intervention(s)—Five week-old mice were treated with a sterilizing busulfan dose and with 7 days of G-CSF or vehicle treatment and evaluated 10 weeks later (experiment 1) or 24 hours after treatment (experiment 2).

Main Outcome Measure(s)—Experiment 1 - testis weights, epididymal sperm counts, testis histology. Experiment 2 - PLZF immunofluorescent co-staining with apoptotic markers. Molecular analysis of G-CSF receptor expression in undifferentiated spermatogonia.

Results—Ten weeks after treatment, busulfan-treated mice that also received treatment with G-CSF exhibited significantly better recovery of spermatogenesis and epididymal sperm counts than animals receiving busulfan alone. G-CSF led to increased numbers of PLZF+ spermatogonia 24 hours after treatment that was not accompanied by changes in apoptosis. To address the cellular

[4]Corresponding Author: Brian P. Hermann, PhD, Address: The University of Texas at San Antonio, One UTSA Circle, San Antonio, TX 78249. Telephone: 210-458-8047, Fax: 210-458-5658, brian.hermann@utsa.edu.
[3]Similar in author order.

Disclosures.
Brian Hermann has a pending US patent 14/177,103 related to the results of this work. The remaining authors have nothing to disclose.

target of G-CSF, mRNA for the G-CSF receptor, *Csf3r*, was found in adult mouse testes and cultured Thy1+ (undifferentiated) spermatogonia, and cell-surface localized CSF3R was observed on 3% of cultured Thy1+ spermatogonia.

Conclusion(s)—These results demonstrate that G-CSF protects spermatogenesis from gonadotoxic insult (busulfan) in rodents and this may occur via direct action on CSF3R +undifferentiated spermatogonia. G-CSF treatment might be an effective adjuvant therapy to preserve male fertility in cancer patients receiving sterilizing treatments.

Keywords

Spermatogonial stem cells; infertility; cancer therapy; fertility preservation; cytokines

Introduction

Lifesaving chemotherapy and radiation treatments for cancer can cause deficits in spermatogenesis that lead to male infertility (1;2). Patients who are making sperm can take advantage of sperm cryobanking before beginning gonadotoxic therapies, which allows for future assisted reproduction using *in vitro* fertilization (IVF) or intracytoplasmic sperm injection (ICSI) (3). By definition, however, prepubertal boys who are not yet producing sperm cannot utilize this approach, and thus, lack options for preserving their future fertility. This is a significant clinical problem because survival rates among childhood cancer patients are nearly 80% (4). Indeed, the American Society of Clinical Oncology recently emphasized the need to provide access to available standard-of-care and experimental fertility preservation approaches for both adult and pediatric patients (5).

Spermatogonial stem cell transplantation is an experimental strategy that regenerates complete spermatogenesis and may restore the fertility of male cancer survivors (6–15). Biopsied testicular tissue obtained prior to sterilizing treatments is cryopreserved so that SSCs present in the tissue may be transplanted back into patients' testes after cancer cure (3;7). Indeed, recent nonhuman primate studies provided definitive demonstration of functional donor spermatogenesis following SSC transplantation using this strategy (14;16). Autologous transplantation, however, carries an inherent risk of reintroducing contaminating malignant cells back into patients after cancer cure (3;10;17) and it is unclear whether this risk can be abated (18–25). Furthermore, since successful nonhuman primate SSC transplants used $46–88\times10^6$ donor cells (14) and human testis tissue yields $42.5–142.8\times10^6$ cells per gram (26–29), human SSC transplant conceivably may require ≥300mg testis biopsies. Since typical testis biopsies of prepubertal patients are miniscule in comparison (≤100mg; [14]), *in vitro* SSC expansion may be necessary for clinical SSC transplantation (3). Moreover, surgical testicular tissue retrieval carries risks associated with anesthesia, infection and delays to primary disease therapy. Thus, while SSC transplantation and related approaches show promise for regenerating spermatogenesis and fertility (30–38), clinical translation may lag until these limitations and risks are addressed. Alternative approaches, such as testicular tissue xenografting or autografting are also the focus of active investigation (reviewed by [23]), but have similar drawbacks and invite new challenges such as mitigating the risk of zoonotic disease transmission (39–41).

Clearly, there is a significant need for less risky and noninvasive approaches to preserve fertility in prepubertal male cancer patients. Here, we demonstrate in mice that treatment with granulocyte colony-stimulating factor (G-CSF) protects spermatogenesis from alkylating chemotherapies. For prepubertal boys (and perhaps some men as well), G-CSF treatment could mean the chance of safely retaining their future fertility after cancer.

Materials and Methods

Animals

Male C57BL/6 mice from Jackson Laboratories were maintained with ad libitum normal laboratory diet. All experiments utilizing animals were approved by the Institutional Animal Care and Use Committee of the University of Texas at San Antonio (Assurance A3592-01) and were performed in accordance with the NIH Guide for the Care and Use of Laboratory Animals.

Experimental design, G-CSF and busulfan treatments

Two experimental schemes were employed. In both, five week old male mice were given seven daily subcutaneous injections of 50ug/kg recombinant human granulocyte colony-stimulating factor (PeproTech) suspended in Dulbecco's PBS (DPBS; Life Technologies) containing 0.5% bovine serum albumin fraction V (MP Biomedicals) or 0.5% BSA in DPBS alone (vehicle). On the third day, mice were also given either busulfan (44 mg/kg, DMSO; Sigma-Aldrich) or DMSO alone by a single IP injection. In experiment 1, animals were euthanized 10 weeks following the last G-CSF/vehicle treatment and testes weights, epididymal sperm counts, testis histololgy were evaluated. In experiment 2, mice were euthanized 24 hours after the last G-CSF/vehicle injection and used for immunofluorescent studies of undifferentiated spermatogonia together with apoptotic measures. See Supplemental Figure 1 for additional information on animal numbers per group in each experiment.

Testis Weights and Histological Analyses

Testes were weighed and fixed with fresh 4% paraformaldehyde, paraffin-embedded and sectioned (5 μm). Testis cross-sections for histological analysis were H&E stained. Composite mosaic images of eight complete sections from each testis (≥35μm between sections) at 20X magnification were generated with an AxioImager M1 (Zeiss) and an AxioCam ICc1 (Zeiss). Round seminiferous tubule cross-sections in each image were categorized according to the degree of spermatogenesis: complete spermatogenesis (all germ cell types up to and including elongating spermatids or spermatozoa), round spermatids (all germ cell types up to and including round spermatids), primary spermatocytes (all germ cell types up to and including primary spermatocytes), empty (marked absence of germ cells, Sertoli cell-only and/or some spermatogonia). Sample sections were blinded for imaging and analysis. Statistically significant differences between groups ($p<0.05$) were determined by Tukey-Kramer ANOVA.

Automated image processing to determine seminiferous tubule morphology was performed using MATLAB 2013b (The MathWorks, Inc). Each composite image was normalized using

adaptive histogram equalization to remove variability between images. Seminiferous tubule cross-sections were segmented using the following automated procedure. Otsu's Method (42) was used to convert the red-green-blue image to a binary image using equally-weighted intensity values for red and blue channels. Objects smaller than 20,000 pixels corresponding to connective and interstitial tissues/cells were disregarded. Morphological operations were used to remove histological artifacts, specifically closing, opening, and hole filling (43) in that order. Subsequently, a Euclidean distance matrix was computed for each pixel (44) and a label matrix was generated using a watershed algorithm (45), producing a label matrix with an integer assigned to each contiguous group of pixels indicating that that group of pixels belonged to a given tubule cross-section. Geometric characteristics were then measured using the *regionprops*() function yielding the cross-sectional area, perimeter, lengths of the major and minor axes, and equivalent diameter ($\sqrt{(4\text{area}/\pi)}$; diameter of a circle with the equivalent area of the object) of each tubule cross-section. Only data from round seminiferous tubule cross-sections [shape factor ($4\pi\text{area}/\text{circumference}^2$) values of ≥ 0.8] were used for subsequent analyses, an approach used previously to define roundness of isolated cells (46–48).

Sperm Counts

One epididymis from each animal was used to quantify sperm counts using a swim-up technique 10 weeks after treatment. Briefly, each complete epididymis was minced in room temperature DBPS, incubated at 37°C for 30 minutes to allow motile sperm to swim out of the ducts and sperm number per ml was determined by hemocytometer after PFA fixation.

Immunofluorescent tissue staining

Tissue sections generated from treated mice were stained with antibodies against PLZF, cleaved CASPASE 3 and by TUNEL (49). Briefly, PFA-fixed paraffin-embedded sections were subjected to antigen retrieval in sodium citrate buffer, rinsed, and blocked in antibody diluent. Blocked sections were labeled concurrently with antibodies for PLZF and cleaved CASPASE 3 (Supplemental Table 1), detected by indirect immunofluorescence, and counterstained with 1ug/ml Hoechst 33342 (Sigma-Aldrich) to identify nuclei. Positive immunoreactivity was validated by omission of primary antibody. Separately, following PLZF antibody incubation, TUNEL labeling was performed using the TACS® TdT *In Situ* Apoptosis Detection Kit (Trevigen) using Mn^{2+}. Subsequently, PLZF staining was detected as above with addition of 10ug/ml AlexaFluor 488-conjugated streptavidin (Life Technologies) to label for TUNEL and counterstained with Hoechst 33342. Fluorescently stained sections were mounted with FluoromountG (Southern BioTech). Composite tiled mosaic images for each complete section at 20X magnification were generated using an AxioImager M1 (Zeiss) and an AxioCam MRm (Zeiss). The frequency of PLZF+ spermatogonia exhibiting positive staining for cleaved CASPASE 3 and TUNEL in each image was determined using NIH Image J using the Cell Counter plugin. To determine the number of PLZF+ spermatogonia per seminiferous tubule cross-section, the total numbers of PLZF-stained nuclei in round seminiferous tubule cross-sections were divided by the number of round cross-sections. For quantification of PLZF overlap with cleaved Caspase 3 or TUNEL, single-positive cells for each marker and double-positive cells were counted in each entire image (complete testis section).

Thy1+ Spermatogonia Culture

Testes from 6–8day old DBA/2 mice were used to Thy1+ spermatogonia cultures on mitomycin-C treated SNL76/7 (STO) feeders in a defined serum-free medium [53;72;87;88]. Cultured spermatogonia were mechanically disrupted from STO feeders by gentle pipetting, washed with ice-cold DPBS and used for RNA isolation and subsequent RT-PCR or protein isolation and Western blot. For flow cytometry experiments, mechanically-disrupted cells were treated with 0.25% Trypsin-EDTA (Life Technologies) to generate single-cell suspensions, followed by addition of 10% FBS and two washes with Hank's balanced salt solution prior to antibody labeling.

RT-PCR

Testes from adult C57BL/6 mice (n=3), three Thy1+ spermatogonia cultures, and STO feeders were used to isolate total RNA with Trizol reagent (Life Technologies). Complementary DNA was synthesized essentially as described (50) with SuperScript III reverse transcriptase (Life Technologies) and oligo-dT priming. Subsequent PCRs used oligodeoxynucleotide primers against *Csf3r* (51) and *Gapdh* (Supplemental Table 2) with Platinum Taq DNA polymerase (Life Technologies). All PCR reactions were resolved by agarose gel electrophoresis.

Single-cell qRT-PCR

Testes from 6–8dpp DBA/2 mice were used to generate a single-cell suspension of Thy1+ spermatogonia as described [53;72;87;88], which was then used for specific target amplification (STA) qRT-PCR measurement of mRNA levels in individual cells using the C1 Single-Cell Autoprep System and BioMark HD instruments (Fluidigm) essentially as described (52). Briefly, individual Thy1+ spermatogonia were captured on a C1 STA microfluidic array (10–17 um cells) using the Fluidigm C1, stained with the LIVE/DEAD Cell Viability/Cytotoxicity Kit (Life Technologies), imaged on a AxioImager M1 to identify dead and multiple cell captures, and pre-amplified cDNA was generated from each cell using the Single Cells-to-CT Kit (Life Technologies), pooled qPCR primers (Supplemental Table 2) and Fluidigm STA reagents according to manufacturer recommendations. Preamplified cDNA was then used for high-throughput qPCR measurement of each amplicon using a BioMark HD system as described with modifications (53). Briefly, a 2.25 μl aliquot of each amplified cDNA was mixed with 2.5 μl of 2X SsoFast EvaGreen Supermix with Low ROX (Bio-Rad) and 0.25 μl of 20X DNA Binding Dye Sample Loading Reagent (Fluidigm) and each sample mix was then pipetted into one sample inlet in a Dynamic Array IFC chip (Fluidigm). Individual qPCR primer pairs (100uM, Supplemental Table 2) were diluted 1:10 with TE (2.5ul total volume), mixed with 2.5 μl Assay Loading Reagent (Fluidigm), and then individually pipetted into one assay inlet in the same Dynamic Array IFC chip. Subsequent sample/assay loading was performed with an IFC Controller HX (Fluidigm) and qPCR was performed on the BioMark HD real-time PCR reader (Fluidigm) following manufacturer's instructions using standard Fast cycling conditions and melt-curve analysis, generating an amplification curve for each gene of interest in each sample (cell). Data were analyzed using Real-time PCR Analysis software (Fluidugm) with the following settings: curve quality threshold 0.65, linear derivative baseline correction,

automatic thresholding by assay, and manual melt curve exclusion. Cycle threshold (Ct) values for each reaction from live single cells were exported and further analyzed using an R-script package, SINGuLar Analysis Toolset 2.1 (Fluidigm), with a limit of detection of 24 and default outlier exclusion, which generated the violin plots of Log2-transformed Ct values for each gene of interest in the 75 live, single Thy1+ spermatogonia.

Western Blot

Total proteins from liver and testes of adult C57BL/6 mice (n=3) and Thy1+ spermatogonial cultures (n=3) were used for Western blot detection of CSF3R (54). Briefly, proteins (50μg) were resolved by SDS-PAGE, transferred to PVDF membrane (Millipore), blocked, probed with primary antibody (Supplemental Table 1) and detected with horseradish peroxidase-conjugated secondary antibodies and SuperSignal West Pico chemiluminescence (Pierce).

Flow cytometry

Flow cytometry was used to identify cell-surface localization of CSF3R on cultured Thy1+ spermatogonia (24). Briefly, cultured mouse Thy1+ spermatogonia were stained with primary antibodies (Supplemental Table 1) in DPBS containing 10% FBS (DPBS+S) at 1.5 × 10^6 cells/ml. Staining was compared to an isotype control antibody to correct for non-specific binding. Primary antibodies were detected by indirect immunoflourescent staining (Supplemental Table 1). Propidium iodide (0.5μg/ml, BD Biosciences) was added for discrimination of dead cells. Evaluation of antibody staining by flow cytometry was performed using an LSRII flow cytometer (BD).

Immunoflourescent staining of cultures

Cultured Thy1+ spermatogonia were fixed with 1% PFA, washed with DPBS, blocked with antibody diluents, and incubated with primary antibodies (Supplemental Table 1) in antibody diluents and subsequently detected by indirect immunoflourescence and counterstained with 1ug/ml Hoechst 33342 to identify nuclei. Positive immunoreactivity was validated by omission of primary antibody. Images of stained cultured cells were acquired using an AxioVert CFL (Zeiss) and an AxioCam MRc5 (Zeiss).

Results

A previous mouse study revealed that G-CSF promoted retention of ovarian reserve in females treated with alkylating chemotherapy (55). To examine the possibility of a similar fertility-preserving G-CSF effect in males, we performed two separate experiments using 5 week-old C57BL/6 mice in conjunction with sterilizing busulfan treatment. In both experiments, mice were randomly separated into three groups: “Control” animals which received only vehicle injections (DPBS + 0.1% BSA; DMSO), “Busulfan Only” animals which received G-CSF vehicle and busulfan treatment (44mg/kg), and “Busulfan + G-CSF” animals which received G-CSF (50ug/kg/day) in addition to busulfan treatment (Supplemental Figure 1). G-CSF or vehicle (DPBS + 0.1% BSA) injections were given every morning for seven days and busulfan or DMSO injections were given on the afternoon of day 3 (Supplemental Figure 1).

In the first experiment, animals in all three groups were allowed to recover for ten weeks after treatment, which is sufficient to identify regenerated spermatogenesis arising from spermatogonial stem cells (56). Testis weights were significantly reduced in animals from both the Busulfan Only and Busulfan + G-CSF groups, compared with controls, but did not differ significantly between the Busulfan Only and Busulfan + G-CSF groups (Figure 1A). Epididymal sperm counts determined using a swim-up procedure were significantly lower in all busulfan-treated animals (Busulfan Only and Busulfan + G-CSF groups) than in controls ($p=0.029$), but sperm counts per epididymis were significantly higher in Busulfan + G-CSF animals than the Busulfan Only mice ($p=0.036$; Figure 1B). Histological examination of the testes confirmed that unlike control testes, in which nearly all tubule cross-sections contained complete spermatogenesis (Figure 1C, F, I and Supplemental Table 3), many tubule cross-sections were devoid of germ cells in animals treated with busulfan (Busulfan Only and Busulfan + G-CSF groups; Figure 1D–E, G-H, J-K and Supplemental Table 3). However, treatment with G-CSF led to significantly better spermatogenic recovery after busulfan treatment than in Busulfan only group ($p=0.0428$; Figure 1E, H, K and Supplemental Table 3). That is, mice in the Busulfan + G-CSF group had significantly more seminiferous tubules with spermatogenesis and significantly fewer empty seminiferous tubules than animals in the Busulfan Only group (Figure 1 and Supplemental Table 3). Morphometric measurements of seminiferous tubule cross-sections demonstrated a significant reduction in tubule diameter, area, and perimeter in all animals treated with busulfan (Busulfan Only and Busulfan + G-CSF groups; Supplemental Figure 2, Supplemental Table 4). Round seminiferous tubule cross-sections containing complete spermatogenesis in busulfan-treated mice did not differ significantly in their diameter, area or perimeter depending on whether G-CSF was administered, but these tubule cross-sections were smaller than untreated controls by all parameters (Supplemental Figure 2, Supplemental Table 4). Overall, these data suggested G-CSF prevented loss of spermatogenesis after busulfan treatment, so we sought to determine the mechanism behind this apparent protective effect of G-CSF.

For this purpose, in our second mouse experiment we treated 5 week-old animals as before and examined undifferentiated spermatogonia in their testes 24 hours after the last G-CSF or vehicle treatment (Supplemental Figure 1). As expected, busulfan treatment (Busulfan Only & Busulfan + G-CSF groups) induced a significant reduction in the number of PLZF+ spermatogonia per seminiferous tubule cross-section compared with controls (Figure 2A–D and Supplemental Table 5). However, busulfan-treated mice that also received G-CSF had significantly more PLZF+ spermatogonia per tubule cross-section than Busulfan Only animals ($p=0.035$; Figure 2A–D and Supplemental Table 5). Despite increased numbers of PLZF+spermatogonia in the Busulfan +G-CSF group (Figure 2E–H and Supplemental Table 5), the proportions of PLZF+ spermatogonia that were positive for TUNEL were not different between the Busulfan Only and Busulfan + G-CSF groups ($p=0.28$). Likewise, the proportions of PLZF+ spermatogonia that were positive for activated Caspase 3 (Figure 2I–L and Supplemental Table 5) were not different between the Busulfan Only and Busulfan + G-CSF groups ($p=0.38$). Thus, the increased numbers of PLZF+ spermatogonia after busulfan induced by G-CSF treatment is not likely the result of reduced apoptotic rates.

To explore the cellular target of G-CSF in the testis, we examined G-CSF receptor expression (CSF3R; Figure 3). RT-PCR detected *Csf3r* mRNA in adult mouse testes, cultures of Thy1+ mouse spermatogonia (which contain SSCs), but not in SNL76/7 STO feeder cells (STO, [26]; Figure 3A). Further, we detected a band corresponding to CSF3R protein by western blot in testis and Thy1+ mouse spermatogonia (Figure 3B). A prominent band of approximately 75kDa was observed in all three samples and a less-prominent band at approximately 100kDa only in the liver sample. To determine whether *Csf3r* mRNA was present in all or some undifferentiated spermatogonia, we performed single-cell qRT-PCR using Thy1+ spermatogonia isolated from pup mouse testes (Figure 3C). *Csf3r* mRNA was present in 74/75 Thy1+ spermatogonia in a normal distribution similar to other mRNAs present in undifferentiated spermatogonia [*Dazl*, *Ddx4*, *Foxo1*, *Gfra1*, *Sohlh1*, *Sohlh2*, and *Zbtb16* (Plzf)] and "housekeeping" controls (*Actb*, *Gapdh*, and *Rpl7*; Figure 3C). Consistent with these single-cell qRT-PCR results, we also observed immunofluorescent staining for CSF3R protein in nearly all cultured Thy1+ spermatogonia that overlapped with nuclear SALL4 staining, which labels undifferentiated spermatogonia, but not in STO feeder cells underlying the cultured cells [(57;58); Figure 3D–F]. To determine if CSF3R was localized to the plasma membrane of cultured Thy1+ spermatogonia, we also examined staining by flow cytometry. Approximately 3% of cultured Thy1+ spermatogonia exhibited cell-surface labeling with a CSF3R antibody (Figure 3G–H), which is similar to previous reports for the CSF1R in Thy1+ spermatogonia (59). These data suggest that G-CSF might act directly on a subset of undifferentiated spermatogonia through binding to its cell surface receptor, CSF3R.

Discussion

Male infertility is a long-term side effect of childhood cancer treatments and preserving or restoring fertility in these patients is a major research focus (3;7;12). Indeed, experimental strategies are under development to preserve male fertility with testicular tissue surgically retrieved from the patient, stored, and used later to reestablish gamete production (e.g., SSC transplantation, tissue grafting). While promising, these approaches are expensive, clinically complicated, and introduce potentially serious risks to the patient (e.g., anesthesia, malignant cell contamination). An alternative to invasive fertility preservation strategies might be to include an adjuvant drug treatment regimen during and/or around the time of chemotherapy/radiation treatment to protect the germline from gonadotoxic damage and potentially preserve fertility.

Since a previous study in female mouse identified a fertility-preserving effect of G-CSF in animals treated with alkylating chemotherapy (55), we tested whether a similar phenomenon might occur in males. Our first experiment demonstrated that mouse spermatogenesis can be protected from busulfan chemotherapy by treatment with the cytokine granulocyte colony-stimulating factor (G-CSF). While it was clear that G-CSF treatment did not spare all spermatogenesis from loss by busulfan, G-CSF did promote significantly better spermatogenic recovery over busulfan treatment alone. Additional studies will be required to maximize the recovery of spermatogenesis induced by G-CSF treatment after sterilizing chemotherapy. One possibility would be to alter the G-CSF dose. Arguably, the 50μg/kg/day G-CSF dose used here (56), is relatively low dose considering that PBSC mobilization

studies in mice typically involve G-CSF doses of 200–250μg/kg/day (61–63). Higher doses might improve the percentage of spermatogenesis surviving a sterilizing chemotherapeutic insult. Regardless, these observations are consistent with results of a previous study by Kim and colleagues in which mice were treated with G-CSF in conjunction with sub-sterilizing (5Gy) gamma irradiation (60). That study reported a beneficial effect of G-CSF treatment (3 days prior to irradiation) on spermatogonial survival 3 weeks after treatment (60). Taken together, all of these results support the conclusion that G-CSF treatment protects spermatogenesis from cytotoxic insult (busulfan or radiation) in rodents.

Surprisingly, regenerating seminiferous tubules from animals in the Busulfan Only or Busulfan + G-CSF groups were also significantly smaller than those in the Control group. This result suggests that chemotherapy reduced the regenerative capacity of spermatogonial stem cells or diminished the spermatogenic ceiling via an effect at the level of testicular somatic cells (e.g., Sertoli cells, Leydig cells). Thus, future studies examining spermatogonial stem cell quality/robustness, Sertoli cell survival, and testosterone production might clarify the impacts of sterilizing chemotherapy on surviving germ cells and testicular somatic cells.

Gonadotropin suppression was among the first adjuvant approaches to male fertility preservation investigated in rodents and demonstrated enhanced recovery of spermatogenesis from surviving SSCs following chemotherapy and radiation treatments (68–71). However, all but one of seven subsequent clinical trials failed to demonstrate that gonadotropin suppression improved sperm counts in men after chemotherapy [reviewed in (72)]. Thus, positive protective effects of adjuvant fertility-protecting therapies in rodents proved to be a poor predictor of success in humans. In the case of G-CSF, results from previous nonhuman primate studies in which animals received high-dose busulfan chemotherapy might inform upon the potential efficacy of G-CSF adjuvant therapy in humans (8;14). In the first study, adult male rhesus macaques that were given a single dose of busulfan (8–12mg/kg) became azoospermic and failed to recover detectable ejaculated sperm for at least one year after treatment (8). In the second, busulfan treatment (8–11mg/kg) was accompanied by G-CSF-mobilization (Neupogen, 10–20μg/kg/day for six days) of hematopoietic stem cells (HSCs) into the general circulation prior to collection by apheresis for autologous HSC transplant to counteract busulfan myelosuppression and then a single injection of pegylated G-CSF (Neulasta) after HSC reinfusion to promote their engraftment (14). Since some of the animals in this latter study were allogeneic SSC transplant recipients in which the transplants failed (never exhibited any evidence of donor SSC engraftment), all sperm observed in ejaculates after busulfan and G-CSF treatment were only from recovering endogenous spermatogenesis. Failed allogeneic SSC transplant recipient monkeys in this study, which also received G-CSF treatments around the time of busulfan treatment, recovered spermatogenesis as early as 20 weeks after busulfan treatment (14), which is consistent with G-CSF-enhanced recovery of spermatogenesis we report here in mice following sterilizing busulfan treatment. While these data from nonhuman primates are not derived from a single, controlled study, they tend to support the clinical potential of G-CSF as a male fertility preservation agent when combined with our current results in rodents.

Results of our second experiment revealed that the G-CSF effect we observed in the first experiment is likely mediated by increased numbers of PLZF+ undifferentiated spermatogonia shortly after treatment, but the mechanism of this effect remains unclear. It is possible that G-CSF may promote PLZF+ spermatogonial survival to increase the regenerative pool or may later drive their proliferation to promote regeneration. Since G-CSF treatments in the present study were given both before and after busulfan administration, it is not possible to discriminate potential protective effects of G-CSF prior to chemotherapy from any regenerative effects that may emerge from G-CSF action after chemotherapy. In the previous study by Kim and colleagues, G-CSF was given only prior to irradiation (3 days), and thus, it is possible that the protective G-CSF effect we observed here is mediated through an action before busulfan treatment.

Detection of G-CSF receptor (CSF3R) in the mouse testis and in undifferentiated spermatogonia, which contain SSCs, suggests that G-CSF may act directly on the foundation of spermatogenesis in the testis. Results from single-cell qRT-PCR and immunofluorescent staining in cultured cells, which suggested widespread *Csf3r* mRNA and CSF3R protein expression among Thy1+ spermatogonia, conflicted with flow cytometry results indicating only 3% of Thy1+ spermatogonia had cell-surface localized CSF3R protein. It is possible that either only a portion of the CSF3R protein produced in Thy1+ spermatogonia is localized to the cell surface or flow cytometry of trypsinized cells underreports the proportion of CSF3R+ cells due to antigen cleavage by tryspin. In either case, this finding mirrors a previous report that the receptor for CSF1 is present in a subset of undifferentiated spermatogonia, including SSCs, and contributes to their self-renewal (59). Thus, it is possible that G-CSF may also play a role in support of ongoing spermatogenesis which is the subject of future investigations. In hematopoiesis, G-CSF has been defined as a mitogen that drives granulopoiesis (64) and modulator of HSC function (65–67). Paradoxically, G-CSF administration to mice promotes non-cell-autonomous HSC expansion, but also induces their quiescence (67). Thus, it is possible that G-CSF could induce proliferation and/or quiescence among spermatogonia to produce the protective effects revealed in this study, and through this action, may be an effective adjuvant therapy for male fertility preservation. While more studies are needed to optimize G-CSF delivery, maximize its spermatogenic protection and define a mechanism of action, G-CSF adds a new potential tool in the growing repertoire of male fertility preservation strategies for cancer patients.

Conclusions

Mouse spermatogenesis and undifferentiated spermatogonia can be protected from loss following busulfan treatment with granulocyte colony-stimulating factor (G-CSF). G-CSF may contribute to normal spermatogenesis since its receptor is expressed by undifferentiated spermatogonia. There is potential for employing G-CSF treatment clinically to protect male fertility in some cancer patients.

Supplementary Material

Refer to Web version on PubMed Central for supplementary material.

Acknowledgements

The authors thank Drs. Annie Lin and John R. McCarrey for use of instrumentation and the staff of the UTSA LARC for animal care. The authors also acknowledge Dr. Jon Oatley (Washington State University) for advice on Thy1+ spermatogonial culture. These studies were funded by National Institutes of Health grants R00HD062687 and R21HD078916 (Hermann), P30GM092334 (John McCarrey), National Science Foundation Major Research Instrumentation grant 1337513 (Hermann), a UTSA Collaborative Research Seed Grant (Hermann), the Helen Freeborn Kerr Charitable Foundation, and the University of Texas at San Antonio. Some data were generated in the University of Texas Health Science Center at San Antonio (UTHSCSA) Flow Cytometry Shared Resource Facility supported by UTHSCSA, P30CA54174 and UL1RR025767. The funding sources had no role in study design, collection, analysis, or interpretation of data, manuscript writing or the decision to submit for publication.

References

1. Wallace WH, Anderson RA, Irvine DS. Fertility preservation for young patients with cancer: who is at risk and what can be offered? Lancet Oncol. 2005; 6:209–218. [PubMed: 15811616]
2. Mitchell RT, Saunders PT, Sharpe RM, Kelnar CJ, Wallace WH. Male fertility and strategies for fertility preservation following childhood cancer treatment. Endocr Dev. 2009; 15:101–134. [PubMed: 19293606]
3. Clark AT, Phillips BT, Orwig KE. Fruitful progress to fertility: Male fertility in the test tube. Nat Med. 2011; 17:1564–1565. [PubMed: 22146462]
4. Ries, LAG.; Melbert, D.; Krapcho, M.; Mariotto, A.; Miller, BA.; Feuer, EJ., et al. SEER Cancer Statistics Review, 1975–2004. Bethesda, MD: National Cancer Institute; 2007.
5. Loren AW, Mangu PB, Beck LN, Brennan L, Magdalinski AJ, Partridge AH, et al. Fertility preservation for patients with cancer: American Society of Clinical Oncology clinical practice guideline update. J Clin Oncol. 2013; 31:2500–2510. [PubMed: 23715580]
6. Kubota H, Brinster RL. Technology insight: In vitro culture of spermatogonial stem cells and their potential therapeutic uses. Nat Clin Pract Endocrinol Metab. 2006; 2:99–108. [PubMed: 16932264]
7. Brinster RL. Male germline stem cells: from mice to men. Science. 2007; 316:404–405. [PubMed: 17446391]
8. Hermann BP, Sukhwani M, Lin CC, Sheng Y, Tomko J, Rodriguez M, et al. Characterization, cryopreservation and ablation of spermatogonial stem cells In adult rhesus macaques. Stem Cells. 2007; 25:2330–2338. [PubMed: 17585169]
9. Geens M, Goossens E, De BG, Ning L, Van SD, Tournaye H. Autologous spermatogonial stem cell transplantation in man: current obstacles for a future clinical application. Hum Reprod Update. 2008; 14:121–130. [PubMed: 18187526]
10. Schlatt S, Ehmcke J, Jahnukainen K. Testicular stem cells for fertility preservation: preclinical studies on male germ cell transplantation and testicular grafting. Pediatr Blood Cancer. 2009; 53:274–280. [PubMed: 19415740]
11. Ginsberg JP, Carlson CA, Lin K, Hobbie WL, Wigo E, Wu X, et al. An experimental protocol for fertility preservation in prepubertal boys recently diagnosed with cancer: a report of acceptability and safety. Hum Reprod. 2010; 25:37–41. [PubMed: 19861330]
12. Wyns C, Curaba M, Vanabelle B, Van LA, Donnez J. Options for fertility preservation in prepubertal boys. Hum Reprod Update. 2010; 16:312–328. [PubMed: 20047952]
13. Hermann, BP.; Orwig, KE. Translating spermatogonial stem cell transplantation to the clinic. In: Orwig, KE.; Hermann, BP., editors. Male Germline Stem Cells: Developmental and Regenerative Potential. 1 ed. New York, NY: Humana Press; 2011.
14. Hermann BP, Sukhwani M, Winkler F, Pascarella JN, Peters KA, Sheng Y, et al. Spermatogonial stem cell transplantation into rhesus testes regenerates spermatogenesis producing functional sperm. Cell Stem Cell. 2012; 11:715–726. [PubMed: 23122294]
15. Firlej V, Barraud-Lange V, Fouchet P. Stem cell therapy for male infertility takes a step forward. Cell Stem Cell. 2012; 11:585–586. [PubMed: 23122284]
16. Shetty G, Uthamanthil RK, Zhou W, Shao SH, Weng CC, Tailor RC, et al. Hormone suppression with GnRH antagonist promotes spermatogenic recovery from transplanted spermatogonial stem cells in irradiated cynomolgus monkeys. Andrology. 2013; 1:886–898. [PubMed: 24124124]

17. Goossens E, Tournaye H. Is there a clinical future for spermatogonial stem cells? Curr Stem Cell Res Ther. 2007; 2:189–195. [PubMed: 18220902]
18. Fujita K, Ohta H, Tsujimura A, Takao T, Miyagawa Y, Takada S, et al. Transplantation of spermatogonial stem cells isolated from leukemic mice restores fertility without inducing leukemia. Journal of Clinical Investigation. 2005; 115:1855–1861. [PubMed: 15965502]
19. Fujita K, Tsujimura A, Miyagawa Y, Kiuchi H, Matsuoka Y, Takao T, et al. Isolation of germ cells from leukemia and lymphoma cells in a human in vitro model: potential clinical application for restoring human fertility after anticancer therapy. Cancer Res. 2006; 66:11166–11171. [PubMed: 17145860]
20. Geens M, van d V, De BG, Goossens E, Van SA, Tournaye H. The efficiency of magnetic-activated cell sorting and fluorescence-activated cell sorting in the decontamination of testicular cell suspensions in cancer patients. Hum Reprod. 2007; 22:733–742. [PubMed: 17082221]
21. Fujita K, Tsujimura A, Okuyama A. Isolation of germ cells from leukemic cells. Hum Reprod. 2007; 22:2796–2797. [PubMed: 17725988]
22. Geens M, Van de Velde H, De Block G, Goossens E, Tournaye H. Reply: Isolation of germ cells from leukemic cells. Hum Reprod. 2007; 22:2797–2798.
23. Hou M, Andersson M, Zheng C, Sundblad A, Soder O, Jahnukainen K. Immunomagnetic separation of normal rat testicular cells from Roser's T-cell leukaemia cells is ineffective. Int J Androl. 2009; 32:66–73. [PubMed: 17916184]
24. Hermann BP, Sukhwani M, Salati J, Sheng Y, Chu T, Orwig KE. Separating spermatogonia from cancer cells in contaminated prepubertal primate testis cell suspensions. Hum Reprod. 2011; 26:3222–3231. [PubMed: 22016413]
25. Dovey SL, Valli H, Hermann BP, Sukhwani M, Donohue J, Castro CA, et al. Eliminating malignant potential from therapeutic human spermatogonial stem cells. Journal Clinical Investigation. 2013; 123:1833–1843.
26. Nagano M, Patrizio P, Brinster RL. Long-term survival of human spermatogonial stem cells in mouse testes. Fertil Steril. 2002; 78:1225–1233. [PubMed: 12477516]
27. Zohni K, Zhang X, Tan SL, Chan P, Nagano M. CD9 is expressed on human male germ cells that have a long-term repopulation potential after transplantation into mouse testes. Biol Reprod. 2012; 87:27. [PubMed: 22592495]
28. Pacchiarotti J, Ramos T, Howerton K, Greilach S, Zaragoza K, Olmstead M, et al. Developing a clinical-grade cryopreservation protocol for human testicular tissue and cells. Biomed Res Int. 2013; 2013:930962. [PubMed: 23509810]
29. Valli H, Sukhwani M, Dovey SL, Peters KA, Donohue J, Castro CA, et al. Fluorescence-and magnetic-activated cell sorting strategies to isolate and enrich human spermatogonial stem cells. Fertil Steril. 2014; 102:566–580. [PubMed: 24890267]
30. Brinster RL, Avarbock MR. Germline transmission of donor haplotype following spermatogonial transplantation. Proc Natl Acad Sci U S A. 1994; 91:11303–11307. [PubMed: 7972054]
31. Ogawa T, Dobrinski I, Avarbock MR, Brinster RL. Transplantation of male germ line stem cells restores fertility in infertile mice. Nat Med. 2000; 6:29–34. [PubMed: 10613820]
32. Shinohara T, Orwig KE, Avarbock MR, Brinster RL. Remodeling of the postnatal mouse testis is accompanied by dramatic changes in stem cell number and niche accessibility. Proc Natl Acad Sci U S A. 2001; 98:6186–6191. [PubMed: 11371640]
33. Nagano M, Brinster CJ, Orwig KE, Ryu BY, Avarbock MR, Brinster RL. Transgenic mice produced by retroviral transduction of male germ-line stem cells. Proc Natl Acad Sci U S A. 2001; 98:13090–13095. [PubMed: 11606778]
34. Brinster CJ, Ryu BY, Avarbock MR, Karagenc L, Brinster RL, Orwig KE. Restoration of Fertility by Germ Cell Transplantation Requires Effective Recipient Preparation. Biol Reprod. 2003; 69:412–420. [PubMed: 12672656]
35. Honaramooz A, Behboodi E, Megee SO, Overton SA, Galantino-Homer H, Echelard Y, et al. Fertility and germline transmission of donor haplotype following germ cell transplantation in immunocompetent goats. Biol Reprod. 2003; 69:1260–1264. [PubMed: 12801978]

36. Orwig KE, Schlatt S. Cryopreservation and transplantation of spermatogonia and testicular tissue for preservation of male fertility. J Natl Cancer Inst Monogr. 2005; 34:51–56. [PubMed: 15784824]
37. Mikkola M, Sironen A, Kopp C, Taponen J, Sukura A, Vilkki J, et al. Transplantation of normal boar testicular cells resulted in complete focal spermatogenesis in a boar affected by the immotile short-tail sperm defect. Reprod Domest Anim. 2006; 41:124–128. [PubMed: 16519717]
38. Kim Y, Turner D, Nelson J, Dobrinski I, McEntee M, Travis A. Production of donor-derived sperm after spermatogonial stem cell transplantation in the dog. Reproduction. 2008; 136:823–831. [PubMed: 18768666]
39. Brown J, Matthews AL, Sandstrom PA, Chapman LE. Xenotransplantation and the risk of retroviral zoonosis. Trends Microbiol. 1998; 6:411–415. [PubMed: 9807786]
40. Aslam I, Fishel S, Moore H, Dowell K, Thornton S. Fertility preservation of boys undergoing anti-cancer therapy: a review of the existing situation and prospects for the future. Hum Reprod. 2000; 15:2154–2159. [PubMed: 11006191]
41. Geens M, De BG, Goossens E, Frederickx V, Van SA, Tournaye H. Spermatogonial survival after grafting human testicular tissue to immunodeficient mice. Hum Reprod. 2006; 21:390–396. [PubMed: 16311289]
42. Otsu N. A Threshold Selection Method from Gray-Level Histograms. IEEE Transactions on Systems, Man and Cybernetics. 1979; 9:62–66.
43. Soille, P. Morphological Image Analysis: Principles and Applications. Berlin, Heidelberg, Germany: Springer-Verlag; 1999.
44. Maurer CR, Qi RS, Raghavan V. A linear time algorithm for computing exact Euclidean distance transforms of binary images in arbitrary dimensions. Ieee Transactions on Pattern Analysis and Machine Intelligence. 2003; 25:265–270.
45. Meyer F. Topographic Distance and Watershed Lines. Signal Processing. 1994; 38:113–125.
46. Dawson K, Wu CT, Qi XY, Nattel S. Congestive heart failure effects on atrial fibroblast phenotype: differences between freshly-isolated and cultured cells. PLoS ONE. 2012; 7:e52032. [PubMed: 23251678]
47. Prasadam I, Farnaghi S, Feng JQ, Gu W, Perry S, Crawford R, et al. Impact of extracellular matrix derived from osteoarthritis subchondral bone osteoblasts on osteocytes: role of integrinbeta1 and focal adhesion kinase signaling cues. Arthritis Res Ther. 2013; 15:R150. [PubMed: 24289792]
48. Maroto-Morales A, Ramon M, Garcia-Alvarez O, Soler AJ, Fernandez-Santos MR, Roldan ER, et al. Morphometrically-distinct sperm subpopulations defined by a multistep statistical procedure in ram ejaculates: intra- and interindividual variation. Theriogenology. 2012; 77:1529–1539. [PubMed: 22365694]
49. Hermann BP, Sukhwani M, Simorangkir DR, Chu T, Plant TM, Orwig KE. Molecular dissection of the male germ cell lineage identifies putative spermatogonial stem cells in rhesus macaques. Hum Reprod. 2009; 24:1704–1716. [PubMed: 19336441]
50. Hermann BP, Hornbaker KI, Maran RR, Heckert LL. Distal regulatory elements are required for Fshr expression, in vivo. Mol Cell Endocrinol. 2007; 260–262:49–58.
51. Harada M, Qin Y, Takano H, Minamino T, Zou Y, Toko H, et al. G-CSF prevents cardiac remodeling after myocardial infarction by activating the Jak-Stat pathway in cardiomyocytes. Nat Med. 2005; 11:305–311. [PubMed: 15723072]
52. Wu AR, Neff NF, Kalisky T, Dalerba P, Treutlein B, Rothenberg ME, et al. Quantitative assessment of single-cell RNA-sequencing methods. Nat Methods. 2014; 11:41–46. [PubMed: 24141493]
53. Dalerba P, Kalisky T, Sahoo D, Rajendran PS, Rothenberg ME, Leyrat AA, et al. Single-cell dissection of transcriptional heterogeneity in human colon tumors. Nat Biotechnol. 2011; 29:1120–1127. [PubMed: 22081019]
54. Hermann BP, Hornbaker K, Rice DA, Sawadogo M, Heckert LL. In vivo regulation of follicle-stimulating hormone receptor by the transcription factors upstream stimulatory factor 1 and upstream stimulatory factor 2 is cell specific. Endocrinology. 2008; 149:5297–5306. [PubMed: 18566134]

55. Skaznik-Wikiel ME, McGuire MM, Sukhwani M, Donohue J, Chu T, Krivak TC, et al. Granulocyte colony-stimulating factor with or without stem cell factor extends time to premature ovarian insufficiency in female mice treated with alkylating chemotherapy. Fertil Steril. 2013; 99:2045–2054. [PubMed: 23453120]
56. Lu CC, Meistrich ML. Cytotoxic effects of chemotherapeutic drugs on mouse testis cells. Cancer Res. 1979; 39:3575–3582. [PubMed: 476683]
57. Gassei K, Orwig KE. SALL4 Expression in Gonocytes and Spermatogonial Clones of Postnatal Mouse Testes. PLoS ONE. 2013; 8:e53976. [PubMed: 23326552]
58. Hobbs RM, Fagoonee S, Papa A, Webster K, Altruda F, Nishinakamura R, et al. Functional antagonism between Sall4 and Plzf defines germline progenitors. Cell Stem Cell. 2012; 10:284–298. [PubMed: 22385656]
59. Oatley JM, Oatley MJ, Avarbock MR, Tobias JW, Brinster RL. Colony stimulating factor 1 is an extrinsic stimulator of mouse spermatogonial stem cell self-renewal. Development. 2009; 136:1191–1199. [PubMed: 19270176]
60. Kim J, Lee S, Jeon B, Jang W, Moon C, Kim S. Protection of spermatogenesis against gamma ray-induced damage by granulocyte colony-stimulating factor in mice. Andrologia. 2011; 43:87–93. [PubMed: 21382061]
61. Ohdo S, Furukubo T, Arata N, Yukawa E, Higuchi S, Nakano S, et al. Influence of dosing time on pharmacological action of G-CSF in mice. Life Sci. 1998; 62:L163–L168.
62. Han B, Unsinger J, Liu F, Link DC, Bessler M. G-CSF induced progenitor mobilization in mice with PIGA blood cells. Hematol J. 2004; 5:347–352. [PubMed: 15297852]
63. Yannaki E, Athanasiou E, Xagorari A, Constantinou V, Batsis I, Kaloyannidis P, et al. G-CSF-primed hematopoietic stem cells or G-CSF per se accelerate recovery and improve survival after liver injury, predominantly by promoting endogenous repair programs. Exp Hematol. 2005; 33:108–119. [PubMed: 15661404]
64. Panopoulos AD, Watowich SS. Granulocyte colony-stimulating factor: molecular mechanisms of action during steady state and 'emergency' hematopoiesis. Cytokine. 2008; 42:277–288. [PubMed: 18400509]
65. McKinstry WJ, Li CL, Rasko JE, Nicola NA, Johnson GR, Metcalf D. Cytokine receptor expression on hematopoietic stem and progenitor cells. Blood. 1997; 89:65–71. [PubMed: 8978278]
66. Richards MK, Liu F, Iwasaki H, Akashi K, Link DC. Pivotal role of granulocyte colony-stimulating factor in the development of progenitors in the common myeloid pathway. Blood. 2003; 102:3562–3568. [PubMed: 12893769]
67. Schuettpelz LG, Borgerding JN, Christopher MJ, Gopalan PK, Romine MP, Herman AC, et al. G-CSF regulates hematopoietic stem cell activity, in part, through activation of Toll-like receptor signaling. Leukemia. 2014 doi: 10.1038/leu.2014.68.
68. Meistrich ML, Wilson G, Huhtaniemi I. Hormonal treatment after cytotoxic therapy stimulates recovery of spermatogenesis. Cancer Res. 1999; 59:3557–3560. [PubMed: 10446960]
69. Meistrich ML, Wilson G, Kangasniemi M, Huhtaniemi I. Mechanism of protection of rat spermatogenesis by hormonal pretreatment: stimulation of spermatogonial differentiation after irradiation. J Androl. 2000; 21:464–469. [PubMed: 10819455]
70. Udagawa K, Ogawa T, Watanabe T, Yumura Y, Takeda M, Hosaka M. GnRH analog, leuprorelin acetate, promotes regeneration of rat spermatogenesis after severe chemical damage. Int J Urol. 2001; 8:615–622. [PubMed: 11903688]
71. Zhang Z, Shao S, Meistrich ML. The radiation-induced block in spermatogonial differentiation is due to damage to the somatic environment, not the germ cells. J Cell Physiol. 2007; 211:149–158. [PubMed: 17167785]
72. Shetty, G.; Wang, G.; Meistrich, ML. Regenerative potential of spermatogenesis after gonadotoxic therapies. In: Orwig, KE.; Hermann, BP., editors. Male Germline Stem Cells: Developmental and Regenerative Potential. New York: Springer; 2011. p. 179-204.

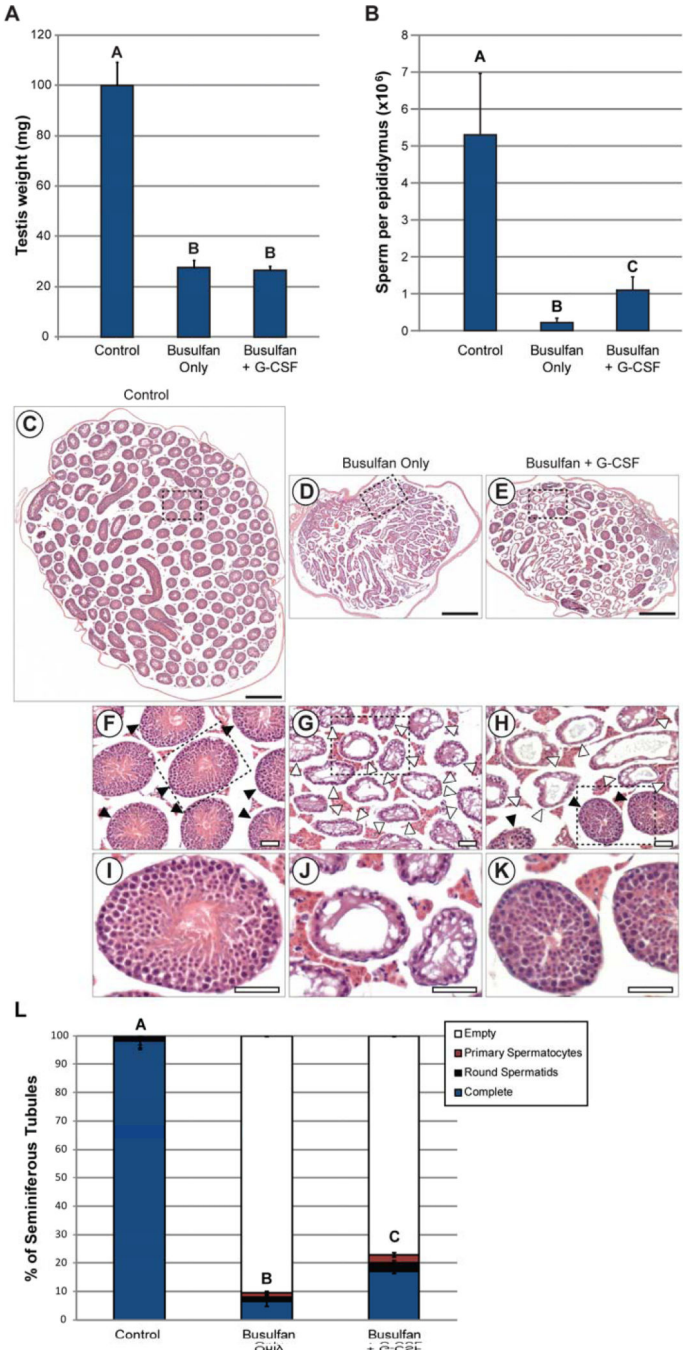

Figure 1. G-CSF prevents loss of spermatogenesis after busulfan treatment in mice

Animals from Experiment 1 were evaluated 10 weeks after the final G-CSF/vehicle treatment (see Supplemental Figure 1). **(A)** Testis weight, **(B)** Epididymal sperm counts. Labels above bars signify statistically-significant differences between groups as determined by student's t-test. Tiled brightfield images of H&E-stained sections of testes from **(C)** Control group, **(D)** Busulfan Only group, and **(E)** Busulfan + G-CSF group. Scale bars = 500μm. Enlarged images of the dashed boxes in C–E are shown in **(F–H)**, respectively. Scale bars = 50μm. Filled arrowheads = seminiferous tubules with spermatogenesis. Open

arrowheads = no spermatogenesis. Further enlarged images of dashed boxes in F–H are shown in **(I–K)**, respectively. Scale bars = 50μm. **(L)** Stacked bars show the percentage of all seminiferous tubule cross-sections counted from all animals in each group which exhibit differing degrees of spermatogenesis: complete spermatogenesis (complete), up to round spermatid spermatids, up to 1° spermatocytes, or containing no spermatogenesis (empty or Sertoli cell-only). A, B, and C categorical notations above bars denote statistically significant differences between groups ($p<0.05$) as determined by Tukey-Kramer ANOVA. The number of animals in each experimental group (n) is indicated at the base of each bar. The number of seminiferous tubule cross-sections evaluated per animal is shown in Supplemental Table 3. Details of experimental groups are in Supplemental Figure 1.

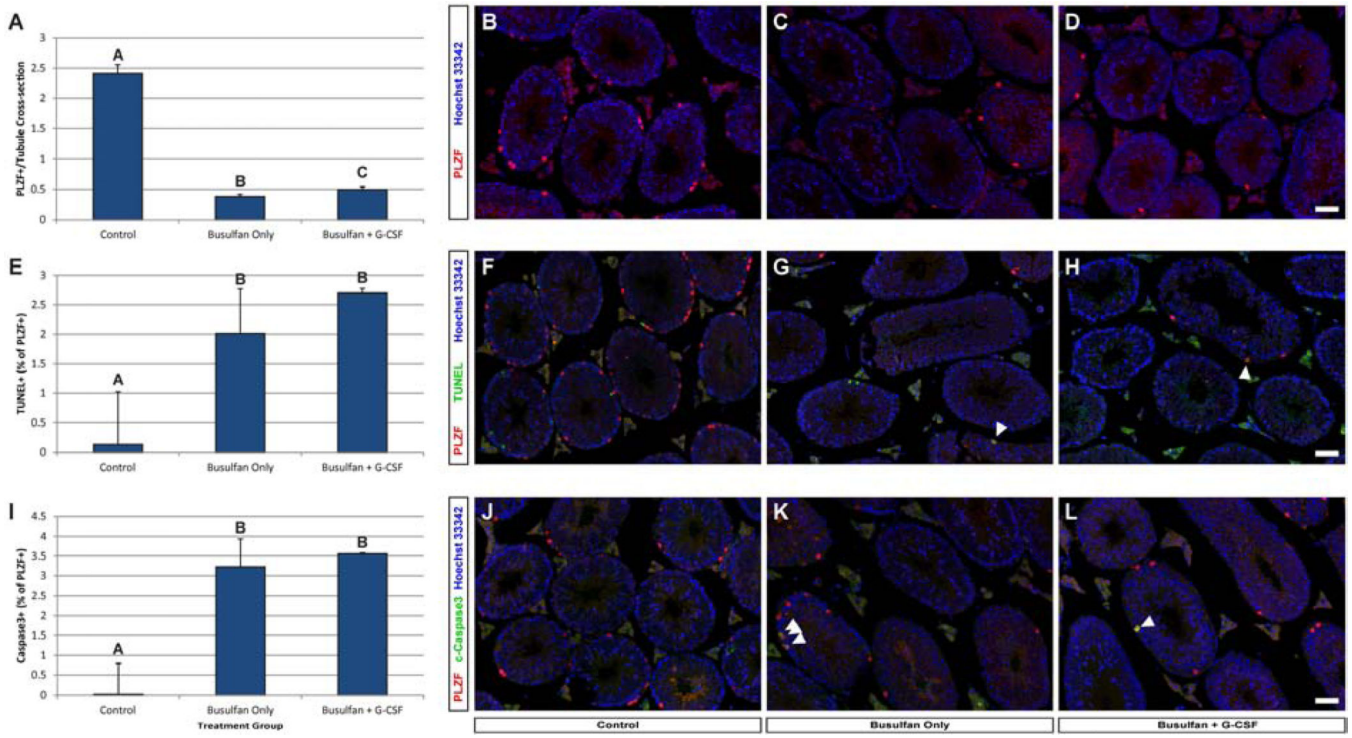

Figure 2. G-CSF treatment improves PLZF+ spermatogonial numbers after busulfan treatment without changing apoptosis

Testes from mice in Experiment 2 were evaluated on day 8 (24 hours after the last G-CSF/vehicle treatment, see Supplemental Figure 1). **(A–D)** PLZF+ spermatogonia were quantifed per round seminiferous tubule cross-section from testes of mice obtained from each group. Sections co-stained for **(E–H)** PLZF and activated Caspase3 or **(I–L)** PLZF and TUNEL were used to determine the percentage of PLZF+ spermatogonia that were positive for activated Caspase 3 and TUNEL, respectively. The A, B, and C categorical notations above bars denote statistically significant differences between groups ($p<0.05$) as determined by Student's T-test. Scale bars = 50μm. The number of round seminiferous tubule cross-sections and cells counted per animal is in Supplemental Table 5.

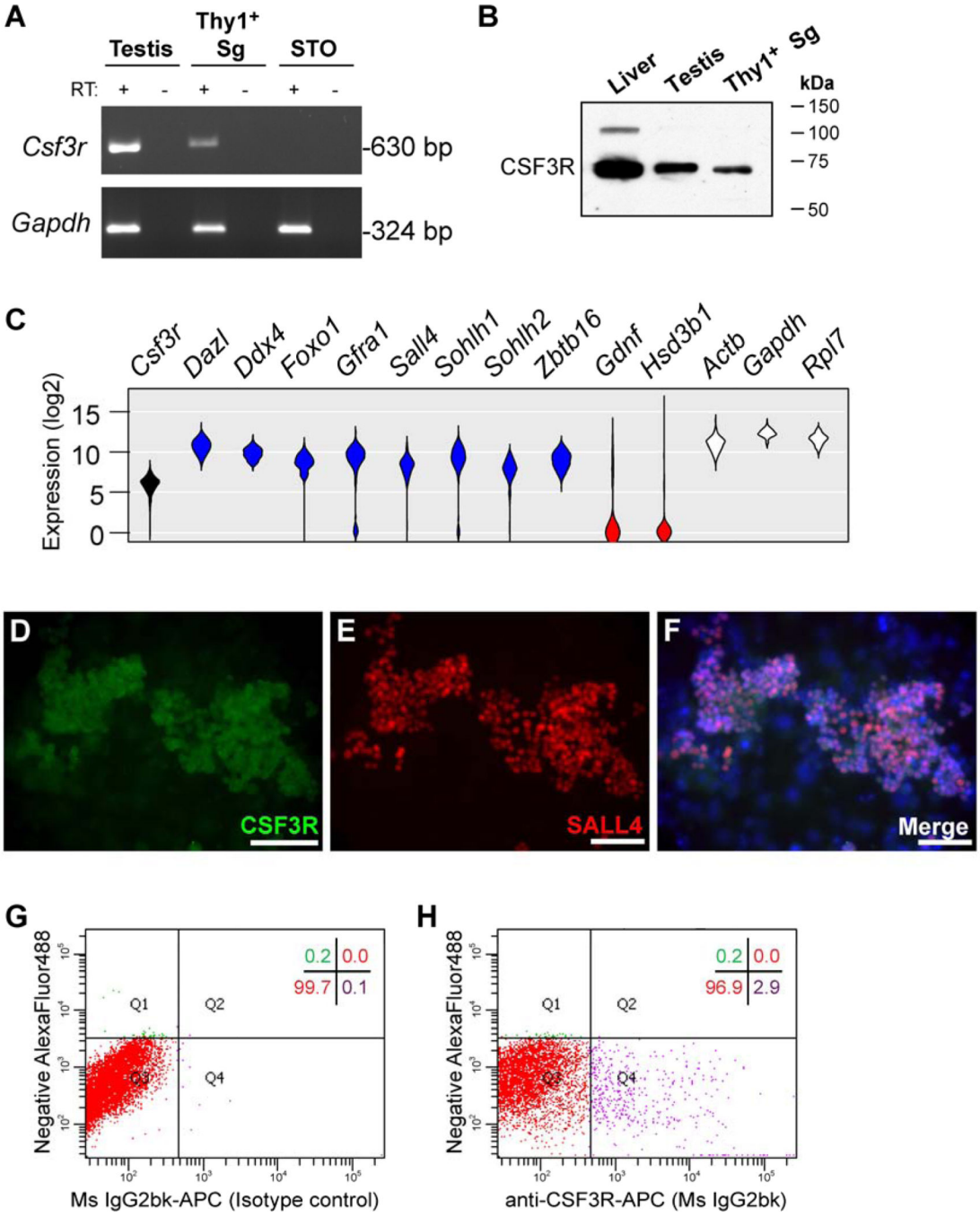

Figure 3. Undifferentiated spermatogonia express CSF3R (G-CSF receptor)

(A) RT-PCR detected mRNAs for **(top)** *Csf3r* and **(bottom)** *Gapdh* in adult mouse testis, cultured Thy1+ spermatogonia and SNL76/7 STO feeders (STO). Template cDNA samples were from reactions with and without reverse transcriptase (RT: + or −). **(B)** Western blot detection of CSF3R in liver (+ control), adult testis and cultured Thy1+ spermatogonia. **(C)** Single-cell qRT-PCR measurement of the steady-state mRNA levels for the noted genes in 75 individual Thy1+ spermatogonia. Data are presented as violin plots of the log2-transformed Ct values from all 75 cells analyzed (curve height = mRNA levels, width =

relative cell number). In addition to *Csf3r* (black), genes were separated into three groups: undifferentiated spermatogonia genes in blue (*Dazl, Ddx4, Foxo1, Gfra1, Sall4, Sohlh1, Sohlh2, and Zbtb16*), somatic cell genes in red (*Gdnf Hsd3b1*), and "housekeeping" control genes in white (*Actb, Gapdh, Rpl7*). Immunofluorescent staining for CSF3R protein in mouse Thy1+ spermatogonia cultures using antibodies that recognize **(D)** CSF3R and **(E)** SALL4, a marker of undifferentiated spermatogonia and **(F)** merged of CSF3R and SALL4 with Hoechst 33342 counterstain (blue, DNA). Staining was compared to omission of primary antibodies (data not shown). Flow cytometry dot plots show Thy1+ spermatogonia cultures stained with **(G)** isotype control antibodies or **(H)** CSF3R antibodies, both on the X-axis. Y-axis depicts autofluorescence in the AlexaFluor488 channel. Quadrant statistics are shown in the upper-right of each dot plot and depict the percentage of propidium iodide (PI) negative (viable) cells that fall within the noted quadrant.